Journal of Sound and Vibration 325 (2009) 597–608

Contents lists available at ScienceDirect

Journal of Sound and Vibration

journal homepage: www.elsevier.com/locate/jsvi

Analysis of the coupled thermoelastic vibration for axially moving beam

Xu-Xia Guo [a,b,*], Zhong-Min Wang [a], Yan Wang [a], Yin-Feng Zhou [a]

[a] School of Sciences, Xi'an University of Technology, 710048 Xi'an, China
[b] Mechanical and Electrical Engineering Department, Baoji University of Arts and Science, 721007 Baoji, China

ARTICLE INFO

Article history:
Received 10 September 2008
Received in revised form
19 March 2009
Accepted 21 March 2009
Handling Editor: L.G. Tham
Available online 22 April 2009

ABSTRACT

The coupled thermoelstic vibration characteristics of the axially moving beam are investigated. The differential equation of motion of the axially moving beam under the thermoelastic coupling is established based to the equilibrium equation and the thermal conduction equation involving deformation term. The eigenequation is deduced and the dimensionless complex frequencies of the axially moving beam with different boundary conditions under the coupled thermoelastic case are calculated by the differential quadrature method. The curves of the real parts and imaginary parts of the first three-order dimensionless complex frequencies versus the dimensionless axially moving speed are obtained. The effects of the dimensionless coupled thermoelastic factor, the ratio of length to height, the dimensionless moving speed on the stability of the beam are analyzed.

1. Introduction

The vibration of the axially moving beams is of considerable interest in many fields. Some examples of the engineering applications include, such as aerial lifter, transmission belt, magnetic tape, band saw and weave fiber. Most of the investigations concerned the transverse vibration characteristics and dynamical behaviors of an axially moving beam. Simpson [1] studied the natural frequencies of the axially moving beam with clamped boundary by the eigenvalue method. Chakraborty and Malik [2] analyzed the linear and nonlinear free vibration of the axially moving beam with simply supported by wave propagation. Kong and Parker [3] researched the free vibration of the axially moving beam with small flexural stiffness, the asymptotic solutions of natural frequencies are obtained by the perturbation method of algebraic equation. Yang [4] studied the natural frequencies of axially moving beams by the method of multiple scales. The above mentioned researches are all in the stable temperature field, the impacts of temperature changes are ignored. But in the actual engineering systems, the impacts of temperature changes need to be taken into consideration. The bending of the beam is inevitably affected by the temperature changes in the elastic vibration, the vibration characteristics and dynamics of the beam will be changed due to the variation of the temperature [5,6]. For this reason, the research of the coupled thermoelastic vibration characteristics for the engineering system components has become a new research field. Owing to the temperature field and the displacement field coupled existed, the thermal conduction equation involving the deformation term and the motion equation must be coupled solved. Chang and Wan [7] studied the nonlinear coupled thermoelastic vibration of the isotropic rectangular thin plate under all kinds of boundary conditions by the Berger

* Corresponding author at: School of Sciences, Xi'an University of Technology, 710048 Xi'an, China.
E-mail address: gxx5432106@sina.com (X.-X. Guo).

0022-460X/$ - see front matter © 2009 Elsevier Ltd. All rights reserved.
doi:10.1016/j.jsv.2009.03.026

assumption. Houston and Photiadis [8] studied the importance of thermoelastic damping for silicon-based MEMS. Eslami and Shakeri [9] analyzed the coupled thermoelastic problems based on the first-order shell theory of the Love assumption. Copper and Pilkey [10] presented a thermoelastic solution technique for beams with arbitrary quasi-static temperature distributions that create large transverse normal and shear stresses. Guo and Rogerson [11] studied the thermoelastic coupling in a doubly clamped elastic prism beam and examined its size-dependence. Sun [12] studied the thermoelastic damping in micro-beam resonators, the results show that the natural frequencies under the thermoelastic coupling are greater than that in case of the uncoupling.

In this paper, the coupled thermoelastic problems of the axially moving beam are studied under the coupled thermoelastic case, the governing equation of thermoelastic coupling Bernoulli–Euler beam is established based on the generalized thermoelastic theory and vibration theory. The eigenequation is obtained, and the dimensionless complex frequencies of the axially moving beam are calculated by the differential quadrature method. The coupled thermoelastic vibration characteristics of the axially moving beam and the effects of the dimensionless coupled thermoelastic factor, the ratio of length to height r and the dimensionless moving speed on the dynamic stability of the coupled thermoelastic axially moving beam are analyzed.

2. Coupled thermoelastic differential equation of axially moving beam

Consider an elastic rectangular beam moving with constant speed v in the x direction, as shown in Fig. 1. The beam has the length L, width b and thickness h in the x, y and z directions, respectively, the density of the material is ρ, the Young's modulus is E.

Denote the initial temperature of the beam as $\tau_0 = \tau(x,z,t_0)$, the temperature of the instantaneous t is $\tau_1 = \tau_1(x,z,t)$, so the temperature changes of the beam is $T = \tau_1 - \tau_0$. The one-dimensional constitutive equation of the beam is

$$\sigma_x = -Ez\frac{d^2 w}{dx^2} - E\alpha_T T \tag{1}$$

where $w = w(x,t)$ is the displacement in the z direction; α_T is the coefficient of linear thermal expansion.

The bending moment of the cross-section is

$$M = -\int_{-h/2}^{h/2} b\sigma_x z\,dz = bE\int_{-h/2}^{h/2}\frac{\partial^2 w}{\partial x^2}z^2\,dz + bE\alpha_T\int_{-h/2}^{h/2} Tz\,dz = EI\frac{\partial^2 w}{\partial x^2} + M_T \tag{2}$$

where $I = bh^3/12$ is the inertia moment of the cross-section; $M_T = bE\alpha_T\int_{-h/2}^{h/2} Tz\,dz$ is the thermal moment.

The equilibrium equation of axially moving beam is [13]

$$\frac{\partial^2 M}{\partial x^2} + \rho A\left(\frac{\partial^2 w}{\partial t^2} + 2v\frac{\partial^2 w}{\partial x\partial t} + v^2\frac{\partial^2 w}{\partial x^2}\right) = 0 \tag{3}$$

where $A = bh$ is the area of the cross-section.

Substituting Eq. (2) into Eq. (3), we can get the thermoelastic equilibrium equation of the beam as follows:

$$EI\frac{\partial^4 w}{\partial x^4} + \frac{\partial^2 M_T}{\partial x^2} + \rho A\left(\frac{\partial^2 w}{\partial t^2} + 2v\frac{\partial^2 w}{\partial x\partial t} + v^2\frac{\partial^2 w}{\partial x^2}\right) = 0 \tag{4}$$

The thermal conduction equation containing the coupled thermoelastic term [14] is

$$\frac{\partial T}{\partial t} - a\left(\frac{\partial^2 T}{\partial x^2} + \frac{\partial^2 T}{\partial z^2}\right) + \frac{E\alpha_T\tau_0}{\rho c_v}\frac{\partial}{\partial t}\left(-z\frac{\partial^2 w}{\partial x^2}\right) = 0 \tag{5}$$

where $a = k/\rho c_v$ is thermal diffusivity; k is the thermal conductivity; c_v is the specific heat at constant volume.

Assuming that there is heat exchange between the upper and lower surfaces of the beam between the surrounding, they belong to convection boundary conditions. The thermal boundary conditions on the upper and lower surfaces of the beam are defined as

$$\left(k\frac{\partial T}{\partial z}\right)_{z=h/2} = H[T_e - (T)_{h/2}] \quad \left(k\frac{\partial T}{\partial z}\right)_{z=-h/2} = -H[T_e - (T)_{-h/2}] \tag{6}$$

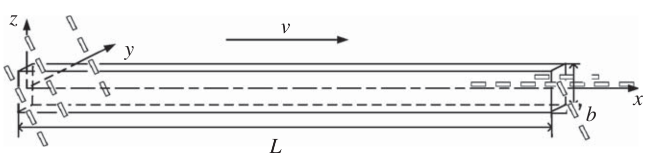

Fig. 1. Axially moving beam in the temperature field.

where T_e is the surrounding temperature changes, and $T_e = 0$; $(T)_{h/2}$ and $(T)_{-h/2}$ denote the temperature changes of the upper and lower surface, respectively; H is the coefficient of the heat exchange by convection, the temperature of the other edges are constant, then

$$\left(\frac{\partial T}{\partial z}\right)_{z=h/2} = -\frac{H}{k}(T)_{h/2} \quad \left(\frac{\partial T}{\partial z}\right)_{z=-h/2} = \frac{H}{k}(T)_{-h/2} \tag{7}$$

Assuming that the temperature varies linearly in the direction of the z axis, one has

$$T = \frac{[(T)_{-h/2} + (T)_{h/2}]}{2} + \frac{[(T)_{h/2} - (T)_{-h/2}]}{h} z \tag{8}$$

Introducing Eq. (8) into Eq. (2), the thermal moment M_T becomes

$$M_T = bE\alpha_T \int_{-h/2}^{h/2} Tz\,\mathrm{d}z = \frac{E\alpha_T bh^2}{12}[(T)_{h/2} - (T)_{-h/2}] \tag{9}$$

Multiplying Eq. (5) by $bE\alpha_T z$, and integrating it with respect to z from $-h/2$ to $h/2$, yields

$$bE\alpha_T \int_{-h/2}^{h/2} \frac{\partial T}{\partial t} z\,\mathrm{d}z - abE\alpha_T \int_{-h/2}^{h/2} \frac{\partial^2 T}{\partial x^2} z\,\mathrm{d}z - abE\alpha_T \int_{-h/2}^{h/2} \frac{\partial^2 T}{\partial z^2} z\,\mathrm{d}z - \frac{E^2\alpha_T^2\tau_0}{\rho c_v} b \int_{-h/2}^{h/2} z^2 \frac{\partial^3 w}{\partial x^2 \partial t}\,\mathrm{d}z = 0 \tag{10}$$

Substituting Eq. (9) into Eq. (10), one obtains

$$\frac{\partial M_T}{\partial t} - a\frac{\partial^2 M_T}{\partial x^2} - abE\alpha_T \int_{-h/2}^{h/2} \frac{\partial^2 T}{\partial z^2} z\,\mathrm{d}z - \frac{E^2\alpha_T^2\tau_0 I}{\rho c_v}\frac{\partial^3 w}{\partial x^2 \partial t} = 0 \tag{11}$$

Consider the Eq. (8) and Eq. (7), $abE\alpha_T \int_{-h/2}^{h/2} (\partial^2 T/\partial z^2) z\,\mathrm{d}z$ in the Eq. (11) can be expressed as

$$\begin{aligned} abE\alpha_T \int_{-h/2}^{h/2} \frac{\partial^2 T}{\partial z^2} z\,\mathrm{d}z &= abE\alpha_T \left[\left(z\frac{\partial T}{\partial z}\right)_{-h/2}^{h/2} - (T)_{-h/2}^{h/2}\right] \\ &= abE\alpha_T \left(\frac{Hh}{2k} + 1\right)[(T)_{-h/2} - (T)_{h/2}] = -\frac{12a}{h^2}\left(\frac{Hh}{2k} + 1\right) M_T \end{aligned} \tag{12}$$

Substituting Eq. (12) into Eq. (11), we can get the thermal conduction equation of the beam as follows:

$$\frac{\partial M_T}{\partial t} - a\frac{\partial^2 M_T}{\partial x^2} + \frac{12a}{h^2}\left(\frac{Hh}{2k} + 1\right) M_T - \frac{E^2\alpha_T^2\tau_0 I}{\rho c_v}\frac{\partial^3 w}{\partial x^2 \partial t} = 0 \tag{13}$$

Now the governing equations for the coupled thermoelastic problem can be obtained by Eq. (4) and Eq. (13) as follows:

$$\begin{cases} EI\dfrac{\partial^4 w}{\partial x^4} + \dfrac{\partial^2 M_T}{\partial x^2} + \rho A\left(\dfrac{\partial^2 w}{\partial t^2} + 2v\dfrac{\partial^2 w}{\partial x \partial t} + v^2\dfrac{\partial^2 w}{\partial x^2}\right) = 0 \\ \dfrac{\partial M_T}{\partial t} - a\dfrac{\partial^2 M_T}{\partial x^2} + \dfrac{12a}{h^2}\left(\dfrac{Hh}{2k} + 1\right) M_T - \dfrac{E^2\alpha_T^2\tau_0 I}{\rho c_v}\dfrac{\partial^3 w}{\partial x^2 \partial t} = 0 \end{cases} \tag{14}$$

For the convenience, the dimensionless quantities are introduced as follows:

$$\xi = \frac{x}{L}, \quad r = \frac{L}{h}, \quad \overline{W} = \frac{w}{h}, \quad \tau = \sqrt{\frac{E}{\rho}}\frac{t}{L}, \quad \overline{M_T} = \frac{M_T}{EAh}, \quad c = \sqrt{\frac{\rho}{E}}v \tag{15}$$

where $\overline{W}$ is the dimensionless deflection, $\overline{M_T}$ is the dimensionless thermal moment.

Substituting Eq. (15) into Eq. (14), we can transform Eq. (14) into the dimensionless form

$$\begin{cases} A_1\dfrac{\partial^4 \overline{W}}{\partial \xi^4} + \dfrac{\partial^2 \overline{M_T}}{\partial \xi^2} + \dfrac{\partial^2 \overline{W}}{\partial \tau^2} + 2c\dfrac{\partial^2 \overline{W}}{\partial \xi \partial \tau} + c^2\dfrac{\partial^2 \overline{W}}{\partial \xi^2} = 0 \\ A_2\dfrac{\partial \overline{M_T}}{\partial \tau} - \dfrac{\partial^2 \overline{M_T}}{\partial \xi^2} + A_3\overline{M_T} - A_4\dfrac{\partial^3 \overline{W}}{\partial \xi^2 \partial \tau} = 0 \end{cases} \tag{16}$$

where $A_1 = 1/12r^2$, $A_2 = L/a\sqrt{E/\rho}$, $A_3 = (12L^2/h^2)((Hh/2k) + 1)$, $A_4 = (\lambda h^2/12La)\sqrt{E/\rho}$, $\lambda = E\alpha_T^2\tau_0/\rho c_v$ is the dimensionless coupled thermoelastic factor.

In order to analyze the vibration characteristics of the beam, we may assume that all quantities change harmonically in Eq. (16), i.e.

$$\overline{W}(\xi,\tau) = W(\xi)\,\mathrm{e}^{\mathrm{j}\omega\tau} \tag{17}$$

$$\overline{M_T}(\xi,\tau) = M_T^*(\xi)\,\mathrm{e}^{\mathrm{j}\omega\tau} \tag{18}$$

where $\mathrm{j} = \sqrt{-1}$, ω is the dimensionless complex frequencies of the coupled thermoelastic axially moving beam.
Substituting Eqs. (17) and (18) into Eq. (16), yields

$$\begin{cases} A_1\dfrac{\mathrm{d}^4W}{\mathrm{d}\xi^4} + \dfrac{\mathrm{d}^2M_T^*}{\mathrm{d}\xi^2} - \omega^2W(\xi) + 2c\mathrm{j}\omega\dfrac{\mathrm{d}W}{\mathrm{d}\xi} + c^2\dfrac{\mathrm{d}^2W}{\mathrm{d}\xi^2} = 0 \\ A_2M_T^*(\xi)\mathrm{j}\omega - \dfrac{\mathrm{d}^2M_T^*}{\mathrm{d}\xi^2} + A_3M_T^*(\xi) - A_4\mathrm{j}\omega\dfrac{\mathrm{d}^2W}{\mathrm{d}\xi^2} = 0 \end{cases} \tag{19}$$

The both ends of the beam, is assumed to be thermally insulated, so the different boundary conditions of the beam are

$$\text{Clamped beam}: \begin{cases} W|_{\xi=0} = W|_{\xi=1} = 0 \\ \left.\dfrac{\mathrm{d}W}{\mathrm{d}\xi}\right|_{\xi=0} = \left.\dfrac{\mathrm{d}W}{\mathrm{d}\xi}\right|_{\xi=1} = 0 \\ M_T^*|_{\xi=0} = M_T^*|_{\xi=1} = 0 \end{cases} \tag{20}$$

$$\text{Simply supported beam}: \begin{cases} W|_{\xi=0} = W|_{\xi=1} = 0 \\ \left.\dfrac{\mathrm{d}^2W}{\mathrm{d}\xi^2}\right|_{\xi=0} = \left.\dfrac{\mathrm{d}^2W}{\mathrm{d}\xi^2}\right|_{\xi=1} = 0 \\ M_T^*|_{\xi=0} = M_T^*|_{\xi=1} = 0 \end{cases} \tag{21}$$

$$\text{Hinged-clamped beam}: \begin{cases} W|_{\xi=0} = \left.\dfrac{\mathrm{d}^2W}{\mathrm{d}\xi^2}\right|_{\xi=0} = 0 \\ W|_{\xi=1} = \left.\dfrac{\mathrm{d}W}{\mathrm{d}\xi}\right|_{\xi=1} = 0 \\ M_T^*|_{\xi=0} = M_T^*|_{\xi=1} = 0 \end{cases} \tag{22}$$

To solve Eq. (19), M_T^* can be derived as follows:

$$M_T^* = \frac{\omega^2W(\xi) + A_4\dfrac{\mathrm{d}^2W}{\mathrm{d}\xi^2}\mathrm{j}\omega - 2c\dfrac{\mathrm{d}W}{\mathrm{d}\xi}\mathrm{j}\omega - c^2\dfrac{\mathrm{d}^2W}{\mathrm{d}\xi^2} - A_1\dfrac{\mathrm{d}^4W}{\mathrm{d}\xi^4}}{A_2\,\mathrm{j}\omega + A_3} \tag{23}$$

We obtain the second derivative of M_T^* from Eq. (23), and introduce it into the first equation in the Eq. (19), yields

$$\begin{aligned} &-A_1\frac{\mathrm{d}^6W}{\mathrm{d}\xi^6} + (A_3A_1 - c^2 + A_1A_2\,\mathrm{j}\omega + A_4\,\mathrm{j}\omega)\frac{\mathrm{d}^4W}{\mathrm{d}\xi^4} - 2c\,\mathrm{j}\omega\frac{\mathrm{d}^3W}{\mathrm{d}\xi^3} \\ &+ (A_3c^2 + A_2c^2\,\mathrm{j}\omega + \omega^2)\frac{\mathrm{d}^2W}{\mathrm{d}\xi^2} + (2cA_3\,\mathrm{j}\omega - 2A_2c\omega^2)\frac{\mathrm{d}W}{\mathrm{d}\xi} - (A_3\omega^2 + A_2\,\mathrm{j}\omega^3)W(\xi) = 0 \end{aligned} \tag{24}$$

Substituting Eq. (23) into Eqs. (20), (21) and (22), the boundary conditions become

$$\text{Clamped beam}: \begin{cases} W|_{\xi=0} = W|_{\xi=1} = 0 \\ \left.\dfrac{\mathrm{d}W}{\mathrm{d}\xi}\right|_{\xi=0} = \left.\dfrac{\mathrm{d}W}{\mathrm{d}\xi}\right|_{\xi=1} = 0 \\ \left.-A_1\dfrac{\mathrm{d}^4W}{\mathrm{d}\xi^4} + (A_4\,\mathrm{j}\omega - c^2)\dfrac{\mathrm{d}^2W}{\mathrm{d}\xi^2}\right|_{\xi=0} = 0 \\ \left.-A_1\dfrac{\mathrm{d}^4W}{\mathrm{d}\xi^4} + (A_4\,\mathrm{j}\omega - c^2)\dfrac{\mathrm{d}^2W}{\mathrm{d}\xi^2}\right|_{\xi=1} = 0 \end{cases} \tag{25}$$

$$\text{Simply supported beam}: \begin{cases} W|_{\xi=0} = W|_{\xi=1} = 0 \\ \left.\dfrac{d^2W}{d\xi^2}\right|_{\xi=0} = \left.\dfrac{d^2W}{d\xi^2}\right|_{\xi=1} = 0 \\ \left.-A_1\dfrac{d^4W}{d\xi^4} - 2c\,j\omega\dfrac{dW}{d\xi}\right|_{\xi=0} = \left.-A_1\dfrac{d^4W}{d\xi^4} - 2c\,j\omega\dfrac{dW}{d\xi}\right|_{\xi=1} = 0 \end{cases} \tag{26}$$

$$\text{Hinged-clamped beam}: \begin{cases} W|_{\xi=0} = \left.\dfrac{d^2W}{d\xi^2}\right|_{\xi=0} = 0 \\ W|_{\xi=1} = \left.\dfrac{dW}{d\xi}\right|_{\xi=1} = 0 \\ \left.-A_1\dfrac{d^4W}{d\xi^4} - 2c\,j\omega\dfrac{dW}{d\xi}\right|_{\xi=0} = 0 \\ \left.-A_1\dfrac{d^4W}{d\xi^4} + (A_4\,j\omega - c^2)\dfrac{d^2W}{d\xi^2}\right|_{\xi=1} = 0 \end{cases} \tag{27}$$

3. Differential quadrature method

Differential quadrature method [15] (DQM) virtually is a method in which the derivatives of the function at the given nodes are approximately described by weighted sums of the function at the total nodes.

Consider a function of one variable $f(x)$, it is continuously differentiable in the interval $[a,b]$. There is a formula

$$L\{f(x)\} = \sum_{j=1}^{N} W_j(x) f(x_j) \tag{28}$$

where L is the linear differential operator, $W_j(x)$ is the interpolation basis functions, x_j is the coordinate value of the node j in the different nodes $a = x_1 < x_2 < \cdots < x_N = b$. If $L = d/dx$, $A_{ij} = W_j(x_i)$ and $f_j = f(x_j)$, then

$$f_i' = \sum_{j=1}^{N} A_{ij} f_j \quad (i = 1, 2, \ldots, N) \tag{29}$$

A_{ij} is the weight coefficients of the first derivative of $f(x)$.

Assuming that $f_i^{[k]} = f^{[k]}(x_i)$ $(i = 1, 2, \ldots, N)$, the higher-order derivatives of the points can be obtained through the function value of the points interpolate as

$$f_i^{[2]} = \sum_{j=1}^{N} B_{ij} f_j, \quad f_i^{[3]} = \sum_{j=1}^{N} C_{ij} f_j, \quad f_i^{[4]} = \sum_{j=1}^{N} D_{ij} f_j, \quad f_i^{[5]} = \sum_{j=1}^{N} E_{ij} f_j, \quad f_i^{[6]} = \sum_{j=1}^{N} F_{ij} f_j \tag{30}$$

where B_{ij}, C_{ij}, D_{ij}, E_{ij} and F_{ij} are the weight coefficients of the first, second, third, fourth, fifth and sixth derivative of $f(x)$.

According the interpolation principle, the weight coefficients of the differential quadrature method are obtained by the differential coefficient of the Lagrange interpolation polynomial on the nodes. A_{ij} can be expressed

$$A_{ij} = \begin{cases} \prod\limits_{\substack{k=1 \\ k\neq i,j}}^{N} (x_i - x_k) \Big/ \prod\limits_{\substack{k=1 \\ k\neq j}}^{N} (x_j - x_k) & (i,j = 1, 2, \ldots, N; i \neq j) \\ \sum\limits_{\substack{k=1 \\ k\neq i}}^{N} \dfrac{1}{(x_i - x_k)} & (i,j = 1, 2, \ldots, N; i = j) \end{cases} \tag{31}$$

After the A_{ij} is determined, B_{ij}, C_{ij}, D_{ij}, E_{ij} and F_{ij} can be expressed as follows:

$$\begin{cases} B_{ij} = \sum\limits_{k=1}^{N} A_{ik}A_{kj}, \;\; C_{ij} = \sum\limits_{k=1}^{N} B_{ik}A_{kj}, \;\; D_{ij} = \sum\limits_{k=1}^{N} C_{ik}A_{kj} \\ E_{ij} = \sum\limits_{k=1}^{N} D_{ik}A_{kj}, \;\; F_{ij} = \sum\limits_{k=1}^{N} E_{ik}A_{kj} \end{cases} \quad (i,j = 1, 2, \ldots, N) \tag{32}$$

The beam with simply supported adopts the weight coefficient method to treat the boundary conditions, and the clamped beam adopts the δ method to treat the boundary conditions. The distribution forms of the nodes are

$$\begin{cases} \zeta_1 = 0,\ \zeta_N = 1,\ \zeta_i = \dfrac{1}{2}\left[1 - \cos\left(\dfrac{2i-3}{2N-4}\pi\right)\right] & (i = 2, 3, \ldots, N-1) \\ \eta_1 = 0,\ \eta_1 = \delta,\ \eta_{N-1} = 1-\delta,\ \eta_N = 1,\ \eta_1 = \dfrac{1}{2}\left[1 - \cos\left(\dfrac{i-2}{N-3}\pi\right)\right] & (i = 3, 4, \ldots, N-2) \end{cases} \tag{33}$$

Then Eq. (24) can be rewritten in the differential quadrature form as

$$\begin{aligned} &A_3A_1\sum_{k=1}^{N} D_{ik}W_k - c^2\sum_{k=1}^{N} D_{ik}W_k - A_1\sum_{k=1}^{N} F_{ik}W_k + A_3c^2\sum_{k=1}^{N} B_{ik}W_k \\ &\quad + \left[A_1A_2\sum_{k=1}^{N} D_{ik}W_k + A_4\sum_{k=1}^{N} D_{ik}W_k - 2c\sum_{k=1}^{N} C_{ik}W_k + 2cA_3\sum_{k=1}^{N} A_{ik}W_k + A_2c^2\sum_{k=1}^{N} B_{ik}W_k\right]\mathrm{j}\omega \\ &\quad + \left[\sum_{k=1}^{N} B_{ik}W_k - A_3W_k - 2A_2c\sum_{k=1}^{N} A_{ik}W_k\right]\omega^2 - A_2\,\mathrm{j}W_k\omega^3 = 0 \quad (i = 2, 3 \ldots N-1) \end{aligned} \tag{34}$$

The differential quadrature forms of boundary conditions (25), (26) and (27) are

$$\text{Clamped beam}: \begin{cases} W_1 = W_N = 0 \\ \sum_{k=1}^{N} A_{2k}W_k = \sum_{k=1}^{N} A_{(N-1)k}W_k = 0 \\ -A_1\sum_{k=1}^{N} D_{3k}W_k + (A_4\,\mathrm{j}\omega - c^2)\sum_{k=1}^{N} B_{3k}W_k = 0 \\ -A_1\sum_{k=1}^{N} D_{(N-2)k}W_k + (A_4\,\mathrm{j}\omega - c^2)\sum_{k=1}^{N} B_{(N-2)k}W_k = 0 \end{cases} \tag{35}$$

$$\text{Simply supported beam}: \begin{cases} W_1 = W_N = 0 \\ \sum_{k=1}^{N} B_{2k}W_k = \sum_{k=1}^{N} B_{(N-1)k}W_k = 0 \\ -A_1\sum_{k=1}^{N} D_{3k}W_k - 2c\,\mathrm{j}\omega\sum_{k=1}^{N} A_{3k}W_k = 0 \\ -A_1\sum_{k=1}^{N} D_{(N-2)k}W_k - 2c\,\mathrm{j}\omega\sum_{k=1}^{N} A_{(N-2)k}W_k = 0 \end{cases} \tag{36}$$

$$\text{Hinged-clamped beam}: \begin{cases} W_1 = \sum_{k=1}^{N} B_{2k}W_k = 0 \\ W_N = \sum_{k=1}^{N} A_{(N-1)k}W_k = 0 \\ -A_1\sum_{k=1}^{N} D_{3k}W_k - 2c\,\mathrm{j}\omega\sum_{k=1}^{N} A_{3k}W_k = 0 \\ -A_1\sum_{k=1}^{N} D_{(N-2)k}W_k + (A_4\,\mathrm{j}\omega - c^2)\sum_{k=1}^{N} B_{(N-2)k}W_k = 0 \end{cases} \tag{37}$$

Eq. (34) and one of the boundary conditions (35), (36) or (37) can be written in the matrix form as

$$\begin{pmatrix} [K_{dd}] & [K_{de}] \\ [K_{ed}] & [K_{ee}] \end{pmatrix}\begin{pmatrix} \{y_d\} \\ \{y_e\} \end{pmatrix} + \omega\begin{pmatrix} 0 & 0 \\ [G_{ed}] & [G_{ee}] \end{pmatrix}\begin{pmatrix} \{y_d\} \\ \{y_e\} \end{pmatrix} + \omega^2\begin{pmatrix} 0 & 0 \\ [R_{ed}] & [R_{ee}] \end{pmatrix}\begin{pmatrix} \{y_d\} \\ \{y_e\} \end{pmatrix} + \omega^3\begin{pmatrix} 0 & 0 \\ 0 & [I] \end{pmatrix}\begin{pmatrix} \{y_d\} \\ \{y_e\} \end{pmatrix} = \begin{pmatrix} 0 \\ 0 \end{pmatrix} \tag{38}$$

Table 1
The first three order dimensionless natural frequencies of the beam under the ambient temperature.

Boundary condition	ω_1	ω_2	ω_3	λ
Clamped	0.6458	1.7802	3.4904	0 (Existing results [12])
	0.6458	1.7798	3.4839	0 (Present solution)
	0.6741	1.8577	3.6260	0.02
	0.7188	1.9791	3.8270	0.05
Simply supported	0.2849	1.1396	2.5639	0 (Existing results [12])
	0.2849	1.1397	2.5656	0 (Present solution)
	0.2974	1.1896	2.6780	0.02
	0.3171	1.2684	2.8554	0.05
Hinged-clamped	0.4451	1.4391	2.9329	0
	0.4646	1.5021	3.0611	0.02
	0.4952	1.5867	3.1535	0.05

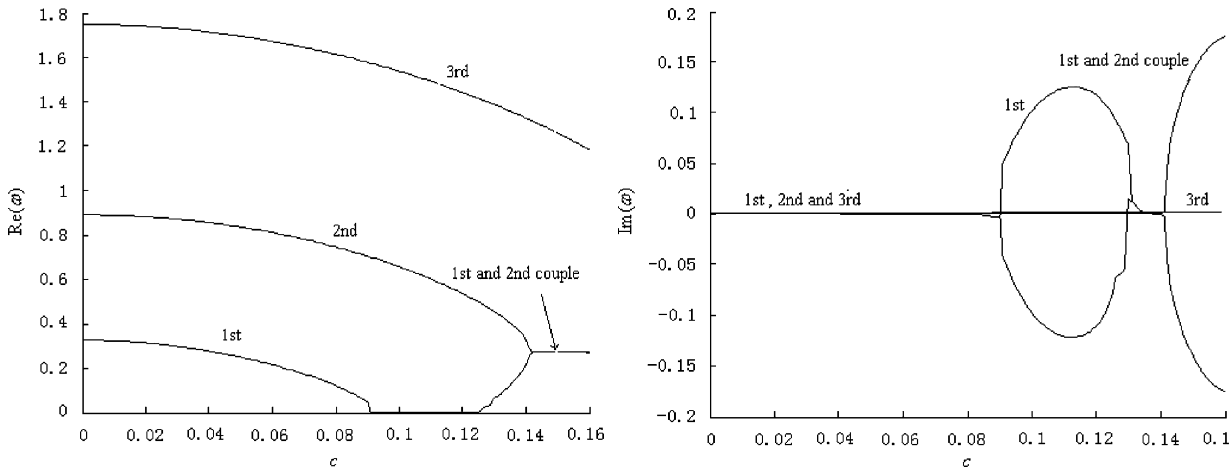

Fig. 2. The first three dimensionless complex frequencies vs. the dimensionless axially moving speed ($r = 20$, $\lambda = 0$).

where the subscript d denotes elements associated with the boundary points, while e is the remainder, namely

$$\{y_d\} = \{y_1, y_2, y_{N-1}, y_N\}^{\mathrm{T}}$$

$$\{y_e\} = \{y_3, y_4, \ldots, y_{N-3}, y_{N-2}\}^{\mathrm{T}} \tag{39}$$

$\{y_d\}$ is eliminated from the Eq. (38), then

$$\{\omega^3[I] + \omega^2[R] + \omega[G] + [K]\}\{W_k\} = \{0\} \tag{40}$$

where the matrix $[K]$, $[G]$, $[R]$ and $[I]$($[I]$ is a $N \times N$ identity matrix when adopts the weight coefficient method to treat the boundary conditions, while adopts the δ method to treat the boundary conditions $[I]$ is a $(N-4) \times (N-4)$ identity matrix), involve several parameters, such as dimensionless axially moving speed c, the dimensionless coupled thermoelastic factor, the ratio of length to height r and so on. Eq. (40) is a generalized eigenvalue problem. Then, the eigenequation of the coupled thermoelastic axially moving beam is

$$|\omega^3[I] + \omega^2[R] + \omega[G] + [K]| = 0 \tag{41}$$

Therefore, one can compute the eigenvalue numerically from Eq. (41) and the natural frequency of the beam with various parameter values.

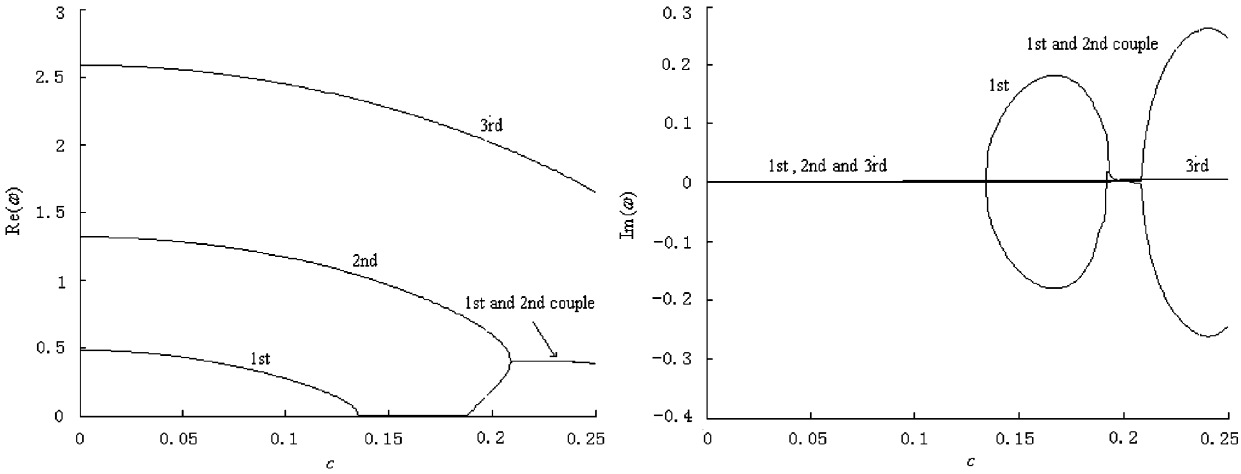

Fig. 3. The first three dimensionless complex frequencies vs. the dimensionless axially moving speed ($r = 20$, $\lambda = 0.1$).

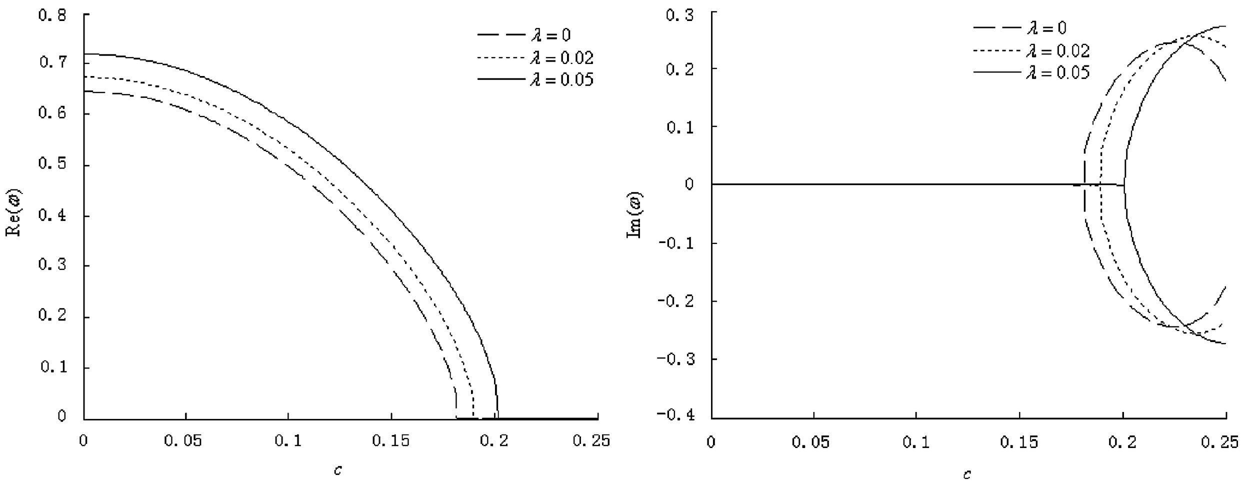

Fig. 4. The first mode dimensionless complex frequencies vs. the dimensionless axially moving speed ($r = 10$).

4. Results and discussions

Numerical studies have been conducted to investigate the effects of several key parameters on the dynamics and stabilities of the coupled thermoelastic axially moving beam. The first three-order natural frequencies of the axially moving beam with different boundary conditions under the $c = 0$, $r = 10$ and the different values of λ were calculated, and the results agree with those exhibited in Ref. [12] under the $\lambda = 0$, which can be seen from Table 1. Here the node number $N = 11$.

4.1. Clamped beam

Fig. 2 shows the variation of the first three-order dimensionless complex frequencies of the beam with the dimensionless moving speed for $r = 20$, $\lambda = 0$. It can be seen that, when the dimensionless moving speed $c = 0$, the dimensionless complex frequency ω is a real number. With the increase of moving speed, the real part of ω decreases, while it's imaginary part remains zero. When the moving speed increases to the critical value $c = 0.091$, the real part of the ω in the first-order mode becomes zero, subsequently $\mathrm{Re}(\omega) = 0$, but $\mathrm{Im}(\omega) > 0$ and $\mathrm{Im}(\omega) < 0$ occur, which shows that the first-order mode becomes unstable by the divergence instability when the moving speed becomes equal or larger than the lowest critical moving speed $c = 0.091$, the lowest critical moving speed is called the divergence speed. For $0.091 < c < 0.125$, the first-order mode is unstable with divergence instability, while the second-order mode and the third-order mode keep stable. When moving speed further increases to $c > 0.125$ the beam regains stability in the first-order mode. After the beam regains stability, in the case of $0.142 < c < 0.16$, the real parts of the first and second-order complex

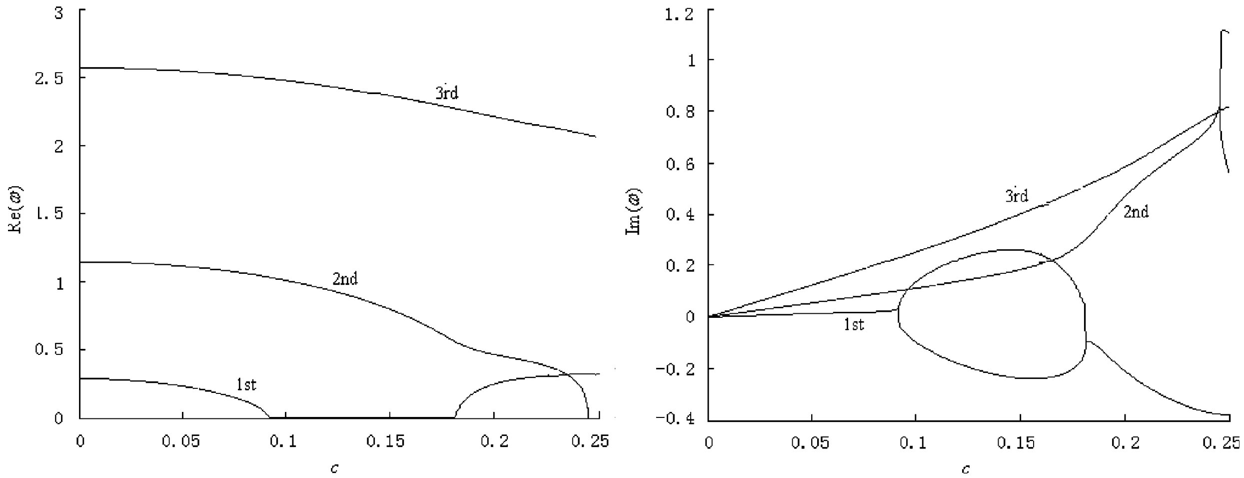

Fig. 5. The first three dimensionless complex frequencies vs. the dimensionless axially moving speed ($r = 10$, $\lambda = 0$).

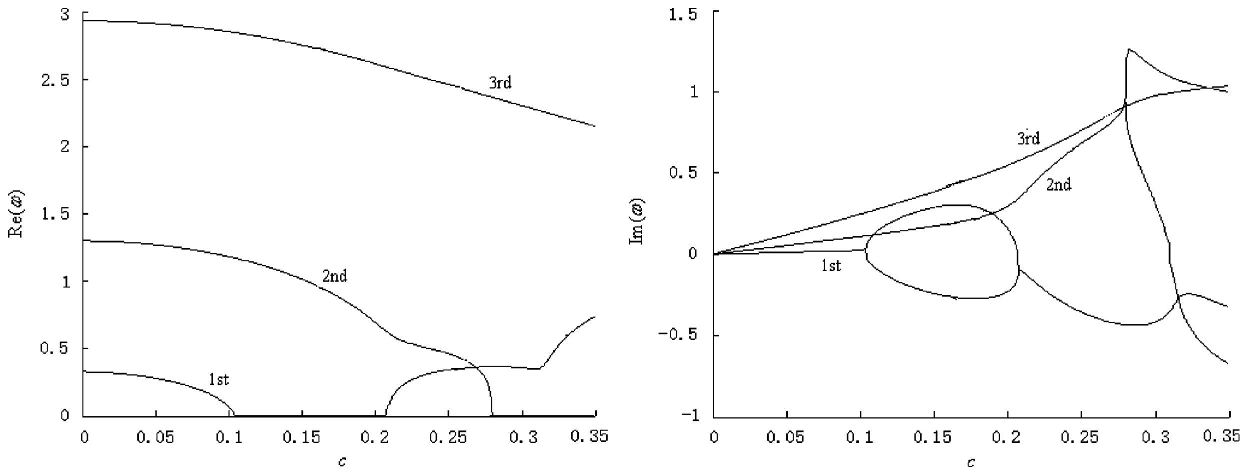

Fig. 6. The first three dimensionless complex frequencies vs. the dimensionless axially moving speed ($r = 10$, $\lambda = 0.1$).

frequencies merge to each other and keep positive, while their imaginary parts become two branches with positive and negative values, it indicates that the first-order mode couples the second-order mode, that is the beam undergoes coupled-mode flutter.

Fig. 3 indicates that the variation of the first three-order dimensionless complex frequencies of the beam with the dimensionless moving speed for $r = 20$, $\lambda = 0.1$. By contrast with Fig. 2, it can be seen that when the dimensionless moving speed $c = 0$, the dimensionless complex frequency ω is also a real number, but they are greater than the values under the $\lambda = 0$ case. The critical speed value of the first-order mode increases to $c = 0.135$ in the Fig. 3, and the beam regains stability in the first-order mode until to the dimensionless moving speed $c = 0.188$. With the increases of the dimensionless moving speed, the first-order mode couples the second-order mode happened.

Fig. 4 shows that the variation of the first-order mode dimensionless complex frequencies of the beam with the dimensionless moving speed for $r = 10$ and the different values of λ. It indicates that the real part of the first-order mode complex frequency increases with the increase of the dimensionless coupled thermoelastic factor when the dimensionless moving speed in the same. The first-order mode behaves divergent instability at the $c = 0.182$ under the $\lambda = 0$. The critical speed of the first-order mode increases with the dimensionless coupled thermoelastic factor λ. In contrast with Fig. 2, the real part of the first-order complex frequency under $r = 10$ is greater than that in the case of $r = 20$.

4.2. Simply supported beam

Figs. 5 and 6 give the variation of the first three-order dimensionless complex frequencies of the beam with the dimensionless moving speed for $r = 10$, $\lambda = 0$ and $\lambda = 0.1$, respectively. In the Fig. 5 one can see that when $c < 0.092$, the real parts of the complex frequencies are reduced until the moving speed increased to the lowest critical moving speed $c=0.092$. Thus, if the moving speed is kept below the lowest critical moving speed, the first three-order mode is always stable. It can be observe that only the real part of the first-order complex frequency becomes zero as the moving speed reaches the lowest critical moving speed while its imaginary part of the first-order complex frequency turns to two different values, it means that the first-order mode becomes unstable. For $0.092<c<0.1803$, the first-order mode behaves divergence instability, while the second and the third-order mode keep stable. For $0.1803<c<0.2483$, the real part of the first-order complex frequency increases while the second and the third keep positive. It is noted that the two values of the imaginary part of the first-order complex frequency merge to each other at $c=0.1803$, the critical moving speed at which the flutter instability occurs in the first mode. This implies in the range $0.1803<c<0.2483$, the second and third modes are always stable, and the first-order mode undergoes flutter instability. However, for $0.2483<c<0.25$, the real part of the second-order complex frequency becomes zero, its imaginary part turns to two different values. Physically this implies that the second-order mode becomes unstable by the divergence instability.

In contrast with Fig. 2, the phenomenon of the first-order mode and second-order mode couple no appear, but the first-order mode and the second-order mode undergo the single-mode flutter, respectively. Fig. 5 compares with Fig. 6, the lowest critical moving speed of the first-mode increases to $c=0.104$ and the second-order mode behaves divergent instability in the case of $c=0.2799$ by the increase of the dimensionless coupled thermoelastic factor λ.

Fig. 7 shows that the variation of the first-order mode dimensionless complex frequencies of the beam with the dimensionless moving speed for $r=20$ and the different values of λ. The real part of the first dimensionless complex frequencies under $c=0$ and the critical speed of the first mode increase with the increase of the dimensionless coupled

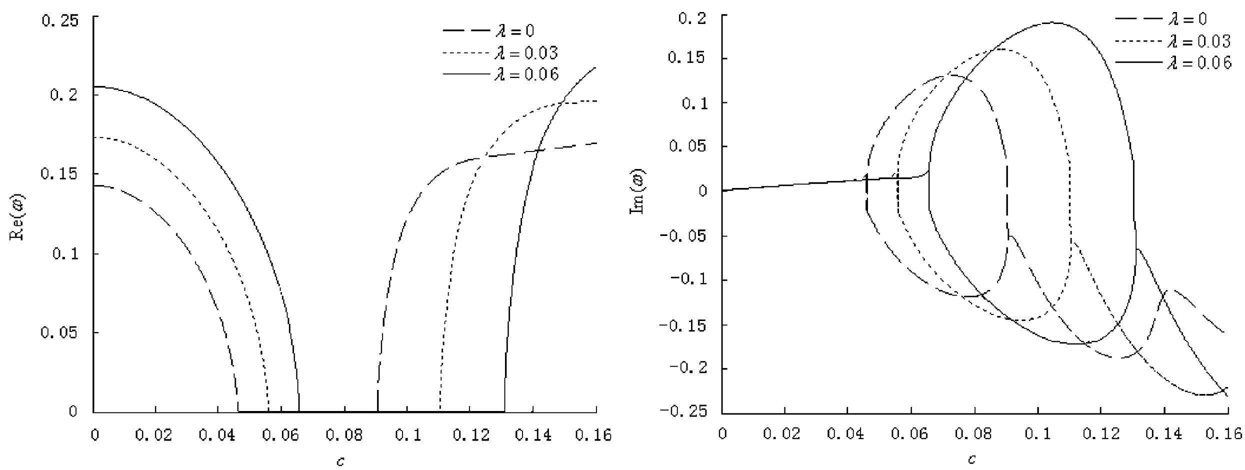

Fig. 7. The first dimensionless complex frequencies vs. the dimensionless axially moving speed ($r=20$).

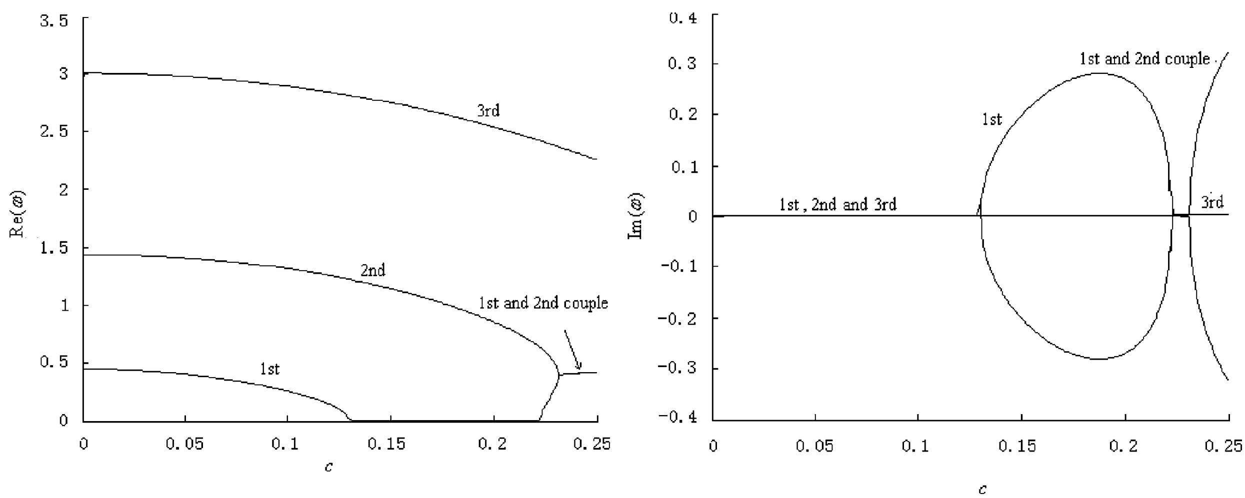

Fig. 8. The first three dimensionless complex frequencies vs. the dimensionless axially moving speed ($r=10$, $\lambda=0$).

thermoelastic factor λ. In comparison with Fig. 5, the real part of the complex frequency in the Fig. 7 is greater than that in the Fig. 5 in the case of $c = 0$ and $\lambda = 0$.

4.3. Hinged-clamped beam

Figs. 8 and 9 indicate that the variation of the first three-order dimensionless complex frequencies of the beam with the dimensionless moving speed for $r = 10$, $\lambda = 0$ and $\lambda = 0.1$, respectively. Fig. 8 indicates that the first-order mode behaves divergent instability at the $c = 0.131$, when the dimensionless moving speed becomes $c = 0.222$, the beam regains stability in the first-order mode. The first-order mode couples the second-order mode until to $c = 0.232$, that is the beam undergoes coupled-mode flutter. In comparison with Figs. 8 and 9, respectively, it is observed that the dimensionless coupled thermoelastic factor $\lambda = 0.1$, the real parts of the dimensionless complex frequencies under $c = 0$ are greater than that in the uncoupled case, so the critical moving speed of the first-order mode increases to $c = 0.149$. The beam undergoes coupled-mode flutter between the first-order mode and the second-order mode in the case of $c = 0.264$.

Fig. 10 gives that the variation of the first-order mode dimensionless complex frequencies of the beam with the dimensionless moving speed for $r = 20$ and the different values of λ. It can be seen that the real part of the dimensionless complex frequencies increase with the increase of the dimensionless coupled thermoelastic factor λ. In comparison with Fig. 8, the real parts of the dimensionless complex frequencies for $r = 20$ are smaller than that for $r = 10$ in the same conditions.

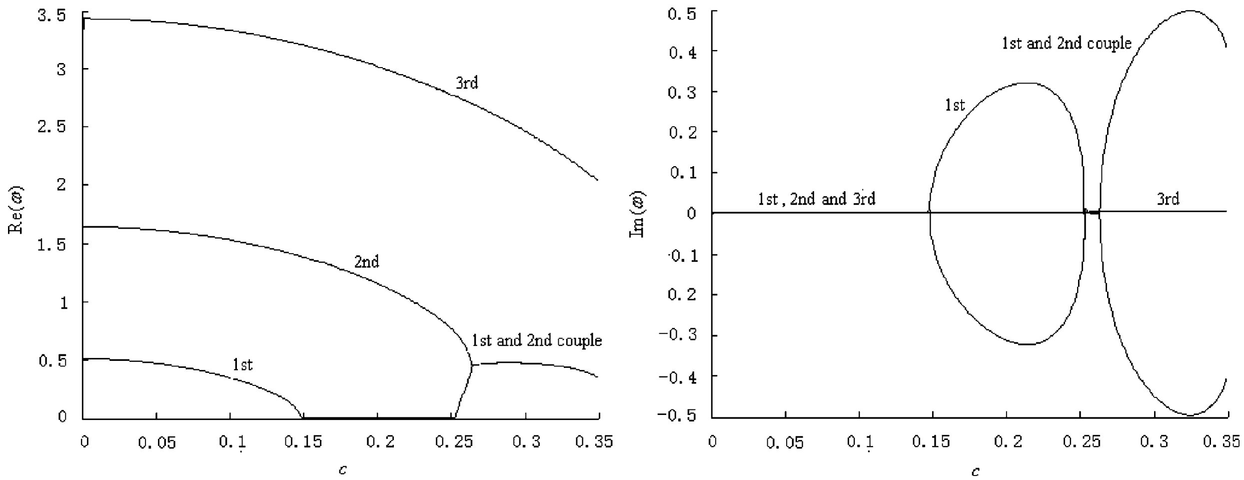

Fig. 9. The first three dimensionless complex frequencies vs. the dimensionless axially moving speed ($r = 10$, $\lambda = 0.1$).

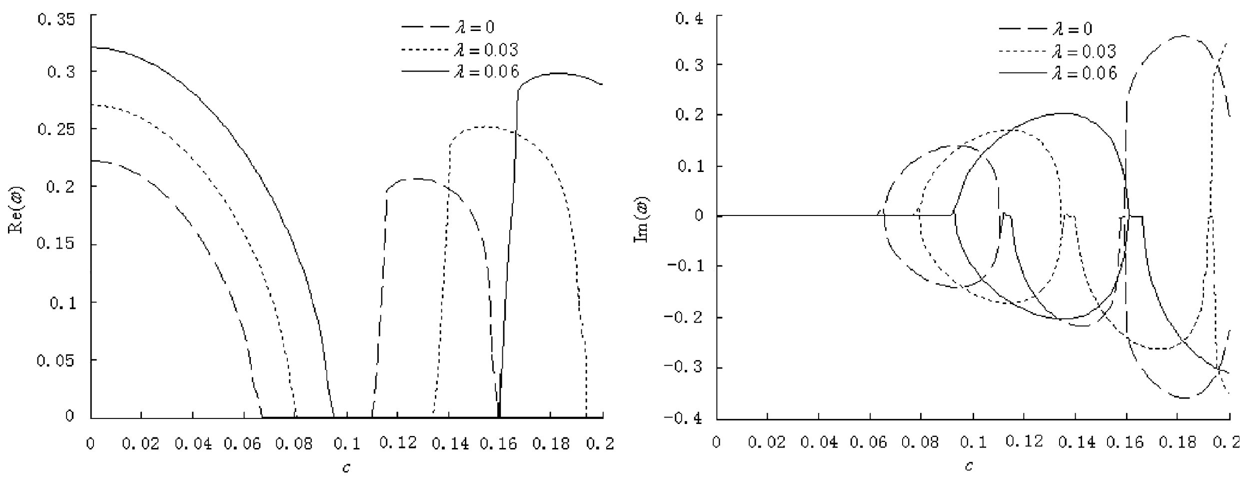

Fig. 10. The first mode dimensionless complex frequencies vs. the dimensionless axially moving speed ($r = 20$).

5. Conclusions

This paper analyzes flutter and divergence instabilities of the coupled thermoelstic axially moving beam, and deduces that the instability type and critical moving speed of the beam are dependent on dimensionless coupled thermoelastic factor λ, the ratio of length to height r and boundary condition. Results of the analysis of the present study can be summarized as follows:

(1) The real parts of the first three complex frequencies of the three kinds of different boundary conditions in the coupled thermoelastic case $\lambda \neq 0$ are greater than that in case of the uncoupling under the other conditions are constants. The critical moving speed of the first-order mode of the moving beam undergoes divergent instability increases with the increase of the dimensionless coupled thermoelastic factor λ.
(2) When other parameters are invariable, with the increase of the ratio of length to height r, the real parts of the first three complex frequencies decrease in the case of $c = 0$, and the critical moving speed of the first-order mode of the moving beam also decreases.
(3) For the three kinds of different boundary conditions, the first modes behave divergent instability firstly, but they are different in the mode which undergoes coupled-mode flutter subsequently. The beam does not exhibit a coupled-mode flutter with simply supported beam, while the clamped and hinged-clamped beam behave the coupled-mode flutter between the first-order mode and second-order mode.

Acknowledgements

The authors gratefully acknowledge the support of the National Natural Science Foundation of China (No. 10872163), the Natural Science Foundation of Education Department of Shaanxi Province of China (No. 08JK394).

References

[1] A. Simpson, Transverse modes and frequencies of beams translating between fixed and supported, *Journal of Mechanical Engineering Science* 15 (3) (1973) 159–164.
[2] G. Chakraborty, A.K. Mallik, Wave propagation in and vibration of a traveling beam with and without non-linear effects, *Journal of Sound and Vibration* 236 (2) (2000) 277–290.
[3] L. Kong, G. Parker, Approximate eigensolutions of axially moving beams with small flexural stiffness, *Journal of Sound and Vibration* 276 (2) (2004) 459–469.
[4] X.D. Yang, Determination of the natural frequencies of axially moving beams by the method of multiple scales, *Journal of Shanghai University* 11 (3) (2007) 251–254.
[5] J. Avsec, M. Oblak, Thermal vibrational analysis for simply supported beam and clamped beam, *Journal of Sound and Vibration* 308 (3) (2007) 514–525.
[6] M. Emil, R. Pedro, Coupled, thermoelastic, large amplitude vibrations of Timoshenko beams, *International Journal of Mechanical Sciences* 46 (2004) 1589–1606.
[7] W.P. Chang, S.M. Wan, Thermomechanically coupled nonlinear vibration of plates, *Internet Journal of Non-linear Mechanics* 21 (5) (1986) 375–389.
[8] B.H. Houston, D.M. Photiadis, J.F. Vignola, M.H. Marcus, X. Liu, D. Czaplewski, L. Sekaric, J. Butler, P. Pehrsson, J.A. Bucaro, Loss due to transverse thermoelastic currents in microscale resonators, *Material Science Engineering A* 370 (1) (2004) 407–411.
[9] M.R. Eslami, M. Shakeri, R. Sedaghati, Coupled thermoelasticity of axially symmetric cylindrical shell, *Journal of Thermal Stresses* 17 (1) (1994) 115–135.
[10] C.D. Copper, W.D. Pilkey, Thermoelasticity solutions for straight beams, *Journal of Applied Mechanics* 69 (5) (2002) 224–229.
[11] F.L. Guo, G.A. Rogerson, Thermoelastic coupling effect on a micro-machined beam resonator, *Mechanics Research Communications* 30 (6) (2003) 513–518.
[12] Y.X. Sun, D.N. Fang, K.S. Ai, Thermoelastic damping in micro-beam resonators, *International Journal of Solids and Structures* 43 (10) (2006) 3213–3229.
[13] L.Q. Chen, Analysis and control of transverse vibrations of axially moving strings, *ASME Applied Mechanics Reviews* 58 (2) (2005) 91–116.
[14] Z.D. Yan, H.L. Wang, *Thermal Stress [M]*, Higher Education Press, Beijing, 1993.
[15] Z.M. Wang, Y.F. Zhou, Y. Wang, Dynamic stability of a non-conservative viscoelastic rectangular plate, *Journal of Sound and Vibration* 307 (1) (2007) 259–264.